Gemcitabine plus nivolumab with carboplatin or oxaliplatin in cisplatin-ineligible patients with metastatic urothelial carcinoma: a randomized phase II trial

Ziao Li[1], Sudeh Izadmehr[1], Jeannie Hoffman-Censits[2], Benjamin Maughan[3], Tina Mayer[4], Alan Tan[5], Rachel Brody[6,7], Hui Xie[8], Kai Nie[8], Geoffrey Kelly[8], Giorgio Ioannou[6,9,13], Rafael Cabal[6,9,13], Kevin Tuballes[6,9,13], Ruiwei Guo[6,9,13], Igor Figueiredo[6,9,13], Diane M. Del Valle[6,9,13], Reza Mehrazin[10], Menggang Yu[11], Qianqian Zhao[12], Seunghee Kim-Schulze[6,8,9,13], John P. Sfakianos[10], Santosh Gupta[14], Noah M. Hahn[15], Edgar Gonzalez-Kozlova[6,9,13,16], Sacha Gnjatic[1,6,7,8,9,13,16#], Matthew D. Galsky[1,6#]

[1]Division of Hematology and Medical Oncology, Icahn School of Medicine at Mount Sinai, New York, NY, USA
[2]Department of Medical Oncology and Department of Urology, The Sidney Kimmel Comprehensive Cancer Center at Johns Hopkins, Baltimore, MD, USA
[3]Huntsman Cancer Institute, University of Utah, Salt Lake City, UT, USA
[4]Department of Medical Oncology, Rutgers Cancer Institute of New Jersey, New Brunswick, NJ, USA
[5]Department of Medicine, Vanderbilt University Medical Center, Nashville, TN, USA
[6]Tisch Cancer Institute, Icahn School of Medicine at Mount Sinai, New York, NY, USA
[7]Department of Pathology, Tisch Cancer Institute, Icahn School of Medicine at Mount Sinai, New York, NY, USA
[8]Human Immune Monitoring Center, Icahn School of Medicine at Mount Sinai, New York, NY, USA
[9]Precision Immunology Institute, Icahn School of Medicine at Mount Sinai, New York, NY, USA
[10]Department of Urology, Tisch Cancer Institute, Icahn School of Medicine at Mount Sinai, New York, NY, USA
[11]Department of Biostatistics, University of Michigan School of Public Health, Ann Arbor, MI, USA
[12]Department of Biostatistics and Medical Informatics, University of Wisconsin Carbone Cancer Center, Madison, WI, USA
[13]Department of Immunology and Immunotherapy, Icahn School of Medicine at Mount Sinai, New York, NY, USA
[14]Translational Research, Epic Sciences Inc, San Diego, CA, USA
[15]Departments of Oncology and Urology, Johns Hopkins University School of Medicine, Baltimore, MD, USA
[16]Department of Oncological Sciences, Tisch Cancer Institute, Icahn School of Medicine at Mount Sinai, New York, NY, USA
[#]These authors contributed equally.

Running title: Different platinum backbones combined with nivolumab in mUC

Addresses for correspondence:
Matthew D. Galsky, MD
Tisch Cancer Institute
Icahn School of Medicine at Mount Sinai
New York, NY 10029
matthew.galsky@mssm.edu

Sacha Gnjatic, PhD
Human Immune Monitoring Center
Icahn School of Medicine at Mount Sinai
New York, NY 10029
sacha.gnjatic@mssm.edu

Conflict of interest disclosure statement: **M.D. Galsky** has received research funding from Bristol Myers Squibb, Novartis, Dendreon, AstraZeneca, Merck and Genentech. He has served as a consultant to Bristol Myers Squibb, Merck, Genentech, AstraZeneca, Pfizer, EMD Serono, SeaGen, Janssen, Numab, Dragonfly, GlaxoSmithKline, Basilea, UroGen, Rappta Therapeutics, Alligator, Silverback, Fujifilm, Curis, Gilead, Bicycle, Asieris, Abbvie and Analog Devices. **S. Gnjatic** received research funding as co-investigator from Boehringer Ingelheim, Bristol Myers Squibb, Genentech, Regeneron and Takeda, and consulting fees from Taiho Pharmaceuticals and Gilead. **J.P. Sfakianos** has served as a consultant or advisor for Natera, Pacific Edge, Merck, Urogen and Janssen. He has served on the speaker bureau for Natera. **N.M. Hahn** has received research funding from AstraZeneca, Incyte, Genentech, Bristol Myers-Squibb, Merck, Loxo Oncology, CG Oncology, Engene, Fidia Farmaceutici, Predicine. He has served as a consultant to Astellas, AstraZeneca, Merck, Tyra Biosciences, Aura Biosciences, Cadence Cancer Research, Cancer Panels, Asieris Pharmaceuticals, EMD Serono, Guidepoint Global, Seattle Genetics, Incyte, Pfizer, Protara Therapeutics, Verity Pharma. He has received speaking honoraria from Medscape. **J. Hoffman-Censits** has received research funding from Sanofi, Genentech, Foundation Medicine, Astellas Pharma, EMD Serono, Seattle Genetics, Daiichi Sankyo, and Ikena Oncology. She has served as a consultant or advisor for Roche/Genentech, Foundation Medicine, AstraZeneca, Seattle Genetics, Gilead Sciences, and Pfizer. She has received speaking honoraria from Roche/Genentech and Clovis Oncology. She has received travel support from Roche/Genentech and Pfizer. She serves on guideline committees for NCCN (Bladder Cancer), AUA (UTUC), and ASCO (GU Cancers).
All remaining authors declare no competing interests.

Word count: 144/150 (translational relevance), 213/250 (abstract), 3578/5000 (text)

Tables and figures: 6/6

References: 30/50

Translational Relevance (144/150 words)

Combining chemotherapy with immune checkpoint inhibitors has improved outcomes across multiple solid tumors, though current approaches typically rely on established cytotoxic "backbones" rather than regimens selected for their immunomodulatory properties. Preclinical studies have demonstrated that oxaliplatin enhances antitumor immunity by inducing immunogenic cell death and increasing immune cell infiltration, making it a promising partner for immune checkpoint blockade. This randomized phase 2 trial evaluated gemcitabine/oxaliplatin and gemcitabine/carboplatin, each combined with nivolumab, in cisplatin-ineligible metastatic urothelial carcinoma patients. The carboplatin-containing regimen achieved a higher response rate. Exploratory biomarker analyses revealed that carboplatin treatment was associated with transcriptional and cellular changes indicative of enhanced adaptive immune activation, whereas oxaliplatin treatment induced signatures consistent with tumor-promoting inflammation. These findings underscore that cytotoxic agents may exert distinct immunomodulatory effects when combined with immune checkpoint blockade and emphasize the critical need to dissect these mechanisms directly in human studies.

Abstract (213/250 words)

Purpose

Oxaliplatin has demonstrated the ability to sensitize tumors to immune checkpoint blockade through its immunomodulatory properties in model systems of cancer. This randomized trial aimed to evaluate gemcitabine/oxaliplatin and gemcitabine/carboplatin, each combined with nivolumab, in cisplatin-ineligible metastatic urothelial carcinoma (mUC) patients.

Patients and Methods

Cisplatin-ineligible patients with mUC were randomized 1:1 to gemcitabine/carboplatin plus nivolumab or gemcitabine/oxaliplatin plus nivolumab for up to 6 cycles, followed by nivolumab monotherapy. A pick-the-winner design was employed with objective response rate (ORR) as the primary endpoint. Secondary endpoints included progression-free survival (PFS) and overall survival (OS). Exploratory analyses evaluated plasma protein analytes, circulating immune cell populations, and circulating tumor cells.

Results

Forty-nine patients were enrolled (carboplatin arm, N = 25; oxaliplatin arm, N = 24). The ORR was 69.6% (95% confidence interval [CI] 0.48–0.87) for the carboplatin arm and 33.3% (95% CI 0.15–0.57) for the oxaliplatin arm. Median OS was 24.74 months and 16.43 months for the carboplatin group and oxaliplatin arms, respectively (hazard ratio 1.99, 95% CI 0.94–4.22; p = 0.07). Exploratory biomarker analyses revealed sustained adaptive immune activation in the carboplatin arm and features suggestive of tumor-promoting inflammation in the oxaliplatin arm.

Conclusions

Oxaliplatin-based chemo-immunotherapy, versus carboplatin-based chemo-immunotherapy, did not yield a higher response rate, challenging assumptions based on preclinical data.

Introduction

Cisplatin-based combination chemotherapy has been a standard-of-care for patients with metastatic urothelial carcinoma (mUC) since the late 1980s. However, approximately 50% of patients are ineligible for cisplatin due to either renal insufficiency or other comorbidities (1–3). In this patient population, carboplatin-based regimens have been used in lieu of cisplatin-based regimens but may be associated with inferior outcomes (4). Optimal regimens for cisplatin-ineligible patients with mUC have historically been a major unmet need.

PD-1/PD-L1 immune checkpoint blockade has transformed the treatment landscape for mUC. As monotherapy, PD-1/PD-L1 inhibitors can induce durable responses, but only in approximately 20–30% of patients (5,6). This limited activity has prompted efforts to expand the benefit of immunotherapy through combination strategies. A widely adopted approach, across multiple tumor types, has been to combine PD-1/PD-L1 blockade with cytotoxic chemotherapy. Chemotherapy can potentially induce immunogenic cell death, promote antigen release, and modulate the tumor microenvironment (TME) in ways that may enhance the efficacy of immune checkpoint blockade (7,8). Despite these potential effects, most clinical trials have combined PD-1/PD-L1 blockade with standard-of-care chemotherapy regimens optimized for direct cytotoxicity, not for their immunomodulatory properties. This conventional strategy may overlook opportunities to potentiate immune responses by selecting cytotoxic agents optimized to potentiate adaptive immunity.

Oxaliplatin is a third-generation platinum compound known to induce immunogenic cell death and stimulate antitumor immunity across multiple model systems of cancer. In contrast to other platinum agents, oxaliplatin has been shown to enhance dendritic cell activation, increase T cell infiltration, and reduce immunosuppressive myeloid populations within the TME predominantly in murine models and *in vitro* cell lines (8,9). These findings suggest that oxaliplatin could serve as a superior cytotoxic backbone for combination regimens with PD-1/PD-L1 blockade.

We hypothesized that cisplatin-ineligible mUC disease setting would be ideal to probe the impact of different cytotoxic regimens combined with immune checkpoint blockade based on the following rationale: (a) a large proportion of patients with mUC are cisplatin ineligible, (b) gemcitabine plus carboplatin has been a standard treatment for such patients, (c) a small phase 2 study previously demonstrated favorable activity with gemcitabine plus oxaliplatin versus gemcitabine plus carboplatin in cisplatin-ineligible patients with mUC (10), and (d) at the time of study design, PD-1/PD-L1 monotherapy was being widely used for this patient population. We therefore conducted a randomized phase 2 trial of gemcitabine/oxaliplatin plus nivolumab and gemcitabine/carboplatin plus nivolumab, in cisplatin-ineligible patients with mUC.

Patients and Methods

Study design

HCRN GU16-287 was an investigator-initiated multi-center randomized open-label phase 2 clinical trial. Patients were enrolled at five participating medical centers (Icahn School of Medicine at Mount Sinai, Johns Hopkins Sidney Kimmel Comprehensive Cancer Center, Huntsman Cancer Institute University of Utah, Rutgers Cancer Institute of New Jersey, and Vanderbilt-Ingram Cancer Center). Patients (described below) were randomized 1:1 to receive either gemcitabine/carboplatin plus nivolumab (Arm A: carboplatin arm) or gemcitabine/oxaliplatin plus nivolumab (Arm B: oxaliplatin arm) for up to 6 cycles in the absence of prohibitive adverse events or disease progression. Patients with at least stable disease at the completion of 6 cycles of combination therapy could continue single-agent nivolumab every 4 weeks for up to 12 cycles. Randomization was done using a centralized web-based system and was stratified by sites of metastatic disease (lymph node–only versus other) via permutated blocks. The trial was registered on clinicaltrials.gov (NCT03451331) and was conducted in compliance with Good Clinical Practice guidelines and all applicable federal, state, or local laws. The study protocol was reviewed and approved by the Institutional Review

Boards at all participating sites, and all patients provided written informed consent prior to enrollment. The full study protocol is available in Supplementary Material.

Patients

Eligible patients were adults aged 18 years or older with histologically documented inoperable, locally advanced or metastatic urothelial carcinoma, for which no prior systemic therapy was administered. Patients were cisplatin ineligible as defined by at least one of the following: calculated creatinine clearance ⩾30 but ⩽60 mL/min, Eastern Cooperative Oncology Group performance status = 2, or National Cancer Institute Common Terminology Criteria for Adverse Events (CTCAE) v4 Grade ⩾ 2 audiometric hearing loss. Major exclusion criteria included 1) prior treatment with anti-PD-1, anti-PD-L1, anti-CTLA4, or any other antibody or drug specifically targeting T cell co-stimulation or immune checkpoint pathways; 2) concurrent active, known or suspected autoimmune disease; 3) known history of human immunodeficiency virus (HIV) infection or acquired immunodeficiency syndrome (AIDS); 4) solid organ or tissue transplant recipients. Full inclusion/exclusion criteria are available in study protocol (Supplementary Material).

Outcomes

The primary objective of the trial was to estimate objective response rate, as determined by RECIST v1.1, with gemcitabine/carboplatin plus nivolumab and gemcitabine/oxaliplatin plus nivolumab in cisplatin-ineligible patients with mUC. Secondary endpoints included adverse events (AEs) determined by the NCI CTCAE v4, duration of response (DOR), progression-free survival (PFS), and overall survival (OS). Tumor responses were assessed after cycle 3 and cycle 6 during combination therapy, every 3 months during maintenance therapy, or at the time of suspected clinical progression by computed tomography (CT) scan of chest, and CT or magnetic resonance imaging (MRI) of abdomen and pelvis.

Translational analyses

Plasma samples were collected at multiple treatment timepoints (Cycle 1 Day 1, Cycle 2 Day 1, Cycle 3 Day 1, and Cycle 8 Day 1) and analyzed using the Olink Immuno-Oncology panel, which quantifies 92 protein analytes relevant to immune response and tumor biology, following the manufacturer's protocol (a full list of analytes is provided in Supplementary Table 1). The data output from the Olink platform is reported as Normalized Protein Expression (NPX) units, which are log2-transformed values proportional to the underlying protein concentrations; thus, an increase of one NPX unit corresponds to a doubling of the protein concentration in the sample.

Mass cytometry (CyTOF) was performed on peripheral blood mononuclear cells (PBMCs) collected at Cycle 1 Day 1, Cycle 3 Day 1, and Cycle 8 Day 1. The full antibody panel is listed in Supplementary Table 2. All utilized antibodies were either purchased pre-conjugated from Fluidigm (RRID: AB_3717872) or conjugated at the Human Immune Monitoring Center (HIMC, RRID: SCR_027571) of Icahn School of Medicine at Mount Sinai (X8 polymer conjugations kits from Fluidigm). Antibodies conjugated in HIMC were all titrated and validated on healthy donor PBMCs. Data were acquired on a Helios mass cytometer (RRID: SCR_019916) and repeat acquisitions of the same sample were concatenated and normalized with Fluidigm software (RRID: SCR_021055). The resultant FCS files were cleaned, normalized, and demultiplexed with an internal pipeline at the HIMC. Astrolabe was then used for automated computational annotation (Astrolabe Diagnostics). Subsequent analyses were performed with Astrolabe annotated data and statistical modeling with R.

Circulating tumor cells (CTCs) enumeration was performed on whole blood samples collected at Cycle 1 Day 1, Cycle 2 Day 1, and Cycle 3 Day 1. Blood samples were shipped to Epic Sciences and processed and analyzed as previously described (11). Any cell that was $CK^{+}CD45^{-}$ with an intact nucleus was classified as a CTC. $CD45^{-}$ nucleated cells with a CK expression lower than assay threshold, but have cytomorphometric features consistent with

CTCs, were also counted as CTC. CTC enumerations were normalized to blood volume used for assay and the final readout was the number detected per 1mL.

Statistical analyses

The modified full analysis set (mFAS) consisted of all patients who received at least 1 dose of study treatment, and the primary evaluable set consisted of all patients who received at least 1 cycle of study treatment and had their disease re-evaluated. The mFAS population was used for safety analyses. A randomized phase 2 “pick-the-winner” design was employed (12) to identify the regimen with truly higher response rate. Accordingly, the ORR and its associated 95% confidence interval (95% CI) were constructed for both arms without formal hypothesis testing. Treatment-emergent adverse event (TEAE) rates were summarized by frequency tables. All time-to-event endpoints, i.e. DOR, PFS, and OS, were analyzed using Kaplan-Meier method without formal hypothesis testing. Therefore, no *p*-value was reported with clinical data.

With 21 patients per arm and an assumed baseline response rate of 40%, the probabilities of selecting the arm that had a true response rate of 60%, 58%, and 55% were 0.9, 0.88, and 0.83, respectively. The planned sample size per arm was inflated to 24 patients to account for early dropouts or unevaluable patients. More detailed power calculations are tabulated in Supplementary Table 3.

The differential protein expression and cell abundance were analyzed with a generalized linear mixed-effect model strategy to account for repeated measurements and relevant baseline variables. Quality control analyses were first performed on both Olink and CyTOF data to identify low detection and poor sample quality. To identify any underlying biases and assess the effect of relevant baseline variables, the variance profiles and data distributions were explored with the packages variancePartition (RRID: SCR_019204) and Dream (13,14). The variables were verified as linearly independent such that no redundancy was present in the data. Protein expression and cell abundance were thus modeled as a function of treatment group, timepoint, and relevant covariates. Differential expression or

abundance was thereafter performed by applying a contrast matrix to each model. Multiple comparison correction was performed wherever deemed necessary with the Benjamini-Hochberg method. Over-representation analysis of differentially expressed Olink analytes was performed by Enrichr (RRID: SCR_001575) with the whole Olink panel as the background (15). Univariate Cox models were used to estimate the hazard ratios and corresponding 95% CIs for PFS and OS. Landmark analyses were used at Cycle 2 Day 1 and Cycle 3 Day 1. All biomarker analyses were exploratory. Reported *p*-values serve as descriptive measures of evidence and should not be interpreted as results of formal hypothesis testing. All statistical analyses were performed using R version 4.3.

Data availability

All de-identified clinical and exploratory experiment data will be deposited under controlled access via the database of Genotypes and Phenotypes (dbGaP), under PHS accession number phs004060.v1.p1, and are available upon reasonable request to the corresponding author until their release. Additional data underlying the figures are available upon reasonable request to the corresponding author.

Results

Patient characteristics

Between May 2018 and August 2021, 55 patients were screened at the five participating centers. A total of 49 patients were enrolled, of whom 25 were randomized to gemcitabine/carboplatin plus nivolumab (Arm A) and 24 were randomized to gemcitabine/oxaliplatin plus nivolumab (Arm B). The CONSORT diagram is shown in Supplementary Figure 1. Demographic and baseline characteristics of all randomized patients are summarized in Table 1. The median age of both groups was 72 years and approximately 30% of patients in both groups had lymph node–only metastases. The majority of patients had primary urothelial cancers originating in the urinary bladder. More than 60% of patients had

baseline Bellmunt score (16) of 1 in both groups. A summary of the representativeness of the study participants is provided in Supplementary Table 4.

Primary and secondary endpoints analyses

Twenty-three patients from the carboplatin arm and 21 from the oxaliplatin arm were included in the primary efficacy analysis. Objective responses were achieved in 16 (69.6%, 95% CI 0.48–0.87) and 7 (33.3%, 95% CI 0.15–0.57) patients in the carboplatin and oxaliplatin groups, respectively (Table 2). The maximal percentage change of tumor burden from baseline for each patient is illustrated in Figure 1A. The median PFS was 9.4 months (95% CI, 5.62–12.88) in the carboplatin arm and 8.57 months (95% CI, 2.56–10.38) in the oxaliplatin arm (HR 1.46 [95% CI, 0.76–2.82]). The median OS was 24.74 months (95% CI, 17.45–NE) for carboplatin arm and 16.42 months (95% CI, 7.66–28.68) for the oxaliplatin arm (HR 1.99 [95% CI, 0.94–4.23]) (Figure 1B, C). The clinical trajectory for each patient is illustrated in Figure 1D.

Safety

The safety population comprised 23 patients from each arm. The three most common treatment-emergent adverse events (TEAEs) among all patients were anemia (67.4%), decreased platelet count (65.2%), and decreased neutrophil count (58.7%) (Table 3). One death occurred in the oxaliplatin arm; this patient experienced a subdural hematoma secondary to a fall while being thrombocytopenic. Grade 3 or 4 TEAEs occurred in 22 (95.7%) and 21 (91.3%) patients in the carboplatin and oxaliplatin arms, respectively. Overall, the two treatment regimens showed similar safety profiles. No new safety signal was observed.

Exploratory biomarker analyses

Olink analyses were performed at C1D1, C2D1, and C3D1, while CyTOF analyses were performed at C1D1 and C3D1 (Figure 2A). Among the circulating analytes, in both treatment groups, soluble plasma PD-1 (PDCD1) demonstrated the highest upregulation

magnitude (2.1- to 2.8-fold increases) from baseline to Cycle 2 or Cycle 3 (Supplementary Figure 2A–D).

In the carboplatin arm, plasma IFN-γ showed ~2-fold increases from baseline to Cycle 2 or Cycle 3, accompanied by increases in CXCL9, CXCL10, CXCL11 (1.5- to 2.1-fold), and the co-stimulatory molecule CD70 (~1.5-fold). Concurrent increases of IL-10, galectin-9 (Gal-9), and galectin-1 (Gal-1) by approximately 1.2- to 1.9-fold, from baseline to Cycle 2 or Cycle 3 were also observed (Supplementary Figure 2A–B). Enrichment analysis of differentially expressed Olink protein analytes revealed pathways related to T cell proliferation and IFN-γ production, as well as macrophage and myeloid differentiation (Supplementary Figure 2E). Within circulating immune cell populations, two natural killer (NK) cell subsets declined by 24–38% from baseline to Cycle 3 (Supplementary Figure 3A).

In the oxaliplatin arm, increases in decorin (DCN, 1.2-fold), carbonic anhydrase 9 (CAIX, 1.4- to 1.7-fold), angiopoietin-1 receptor (TIE2, 1.3-fold), and nitric oxide synthase 3 (NOS3, ~1.4-fold) (Supplementary Figure 2C–D) were observed from baseline to Cycle 2 or Cycle 3. Enrichment analysis revealed the collective changes in analytes from baseline to post-treatment timepoints represented pathways related to macrophage and myeloid differentiation whereas pathways related to T cell proliferation and IFN-γ production showed attenuated enrichment compared to carboplatin (Supplementary Figure 2E). These changes in plasma analytes by Olink were corroborated by expansions of non-classical (2.5-fold) and intermediate (1.8-fold) monocyte populations from baseline to Cycle 3. Notably, circulating plasmacytoid dendritic cells (pDCs) also showed 2-fold expansion at Cycle 3 (Supplementary Figure 3B).

Between-group analysis further highlighted these diverging patterns. Treatment-induced elevations in plasma IFN-γ levels were approximately 2-fold greater with carboplatin versus oxaliplatin at both Cycle 2 and Cycle 3, whereas oxaliplatin showed greater on-treatment elevations versus carboplatin in IL-6 (2-fold at Cycle 2), TIE2 (~1.2-fold at Cycle 2), and CAIX (1.6-fold at Cycle 3) (Figure 2B–D). Non-classical monocytes expansion in blood was also 2-fold greater at Cycle 3 with oxaliplatin versus carboplatin (Figure 2E–F).

Correlative analyses identified biomarkers associated with objective response. Baseline CXCL9, CXCL10, and CXCL11 (odds ratio [OR] 2.1–2.3) and on-treatment PD-1 at Cycle 2 and Cycle 3 (OR 3.6–5.3) were associated with higher likelihood of response, whereas on-treatment CSF-1 at Cycle 2 (OR 0.06–0.08), tumor necrosis factor receptor super family member 21 (TNFRSF21) at Cycle 2 and Cycle 3 (OR ~0.05), and vascular endothelial growth factor A at Cycle 2 and Cycle 3 (VEGFA, OR 0.2–0.3) were associated with lower likelihood of response. CAIX correlated with higher likelihood of response at both baseline and post-treatment timepoints (Figure 3A–C). Among immune cell blood populations, $CD8^+$ central memory T (T_{CM}) cells at baseline and Cycle 3 (OR 1.4–1.5), and pDCs at Cycle 3 (OR 1.4) positively correlated with response, whereas baseline classical monocytes negatively correlated response (OR 0.56) (Figure 3D–E).

Survival analyses demonstrated that while pre-treatment plasma CSF-1 level was not associated with survival outcomes (Supplementary Figure 4A), its on-treatment elevations were associated with inferior OS at Cycle 2 and Cycle 3 (Supplementary Figure 4B–G). TNFRSF21 similarly demonstrated consistent negative associations with OS (Supplementary Figure 4A–C). Among immune cell blood subsets, higher levels of $CD8^+$ T_{CM} and $CD8^+$ naïve T cells at baseline and Cycle 3 were associated with improved OS (Supplementary Figure 5A–B). Despite CSF-1's negative impact on OS, no monocyte subset showed clear prognostic value (Supplementary Figure 5A–E).

CTC levels increased at Cycle 2 in both groups, primarily driven by a small subset of patients, but subsequently declined by Cycle 3 toward their respective baselines. Neither baseline nor on-treatment CTC levels were notably associated with clinical outcomes (Supplementary Figure 6).

Discussion

Following the observation that PD-1/PD-L1 blockade can induce durable disease control in a subset of patients with metastatic solid tumors, expanding its efficacy has

remained a key focus of research. Given their largely non-overlapping mechanisms of action and toxicity profiles, combinations of cytotoxic chemotherapy with immune checkpoint blockade have been extensively investigated. Despite initial concerns about the possibility that chemotherapy might antagonize immune checkpoint blockade through immune cell depletion, such regimens have now been demonstrated to confer survival benefits across various solid tumors, leading to their adoption as treatment standards (17). Most combinations, however, have relied on well-established cytotoxic backbones rather than exploiting the immunomodulatory properties of certain drugs. At the time this trial was designed, no large dataset had firmly established the clinical benefit of chemo-immunotherapy in mUC.

We conducted a randomized phase 2 "pick-the-winner" trial in which the only varied treatment component was the choice of platinum agent: carboplatin or oxaliplatin. We aimed to examine whether the immunomodulatory effects attributed to oxaliplatin in preclinical studies could translate into improved clinical efficacy when combined with immune checkpoint blockade. Unexpectedly, the carboplatin arm achieved a higher ORR than the oxaliplatin arm. While this result may reflect limited statistical power or potential enrollment imbalances despite randomization, baseline Olink and CyTOF profiling did not reveal evidence of a markedly skewed immune landscape between groups. Furthermore, exploratory biomarker analyses suggested on-treatment changes associated with adaptive immunity were more prominent on the carboplatin arm.

During the conduct of this study, several pivotal randomized trials were published that provide critical context for our findings. Neither IMvigor130 nor KEYNOTE-361, which randomized patients with mUC to gemcitabine plus either cisplatin or carboplatin with or without PD-1/PD-L1 blockade, demonstrated improvements in PFS or OS with the addition of PD-1/PD-L1 blockade to chemotherapy. The ORRs in patients receiving gemcitabine, carboplatin, plus atezolizumab and gemcitabine, carboplatin, plus pembrolizumab in these studies were 42.0% and 47.2%, respectively (18,19). Subgroup analyses from these studies revealed that the benefit of adding PD-1/PD-L1 blockade to chemotherapy might have been limited to patients receiving cisplatin with translational analyses supporting that concept (20).

Indeed, CheckMate 901 trial, which randomized patients to gemcitabine plus cisplatin with or without nivolumab demonstrated a survival benefit with the addition of PD-1 blockade (21). Collectively, these data indicate that our high response rate with gemcitabine, carboplatin, plus nivolumab is likely an overestimate due to the small sample size/patient characteristics but that gemcitabine, oxaliplatin, plus nivolumab is still unlikely to outperform gemcitabine, carboplatin, plus nivolumab in this setting.

More recently, the EV-302 trial established enfortumab vedotin plus pembrolizumab (EV/pembro) as a standard treatment for patients with mUC regardless of cisplatin-eligibility (22). However, several factors limit its displacement of cytotoxic chemotherapy, including drug accessibility, financial burden, and a distinctive toxicity profile (23,24). Furthermore, platinum-based chemotherapy remains clinically relevant in the salvage setting for patients who progress on first-line EV/pembro regimen.

Our exploratory biomarker analyses revealed on-treatment differences in immunomodulatory effects between the arms. In the carboplatin arm, IFN-γ, and the tissue-homing T cell chemokines CXCL9 and CXCL10 increased consistently in plasma after treatment initiation, changes that may indicate enhanced adaptive immune activity at tissue sites. In the oxaliplatin arm, we observed lower IFN-γ induction, along with more pronounced upregulation of analytes linked to angiogenesis and inflammation, including TIE2, NOS3, and IL-6 (25–28). While some of the analytes increased in the oxaliplatin arm were individually linked to higher response rate (e.g., CAIX), the overall effects suggested a shift toward a more immunosuppressive circulating immune cell compartment. Importantly, gemcitabine has also been associated with immunomodulatory effects though was a constant between our two treatment arms.

Our findings differ from the large body of preclinical evidence demonstrating the immunostimulatory effects of oxaliplatin, which are not typically associated with carboplatin. Several factors may account for this discrepancy. First, there are fundamental differences between studies in model systems and more complex and heterogenous human studies. Second, chemotherapy dose and schedule may have impacted our findings. Preclinical

studies often use regimens optimized for immunologic effects, whereas the oxaliplatin-based regimen in our study followed common clinical practice (29,30). Third, the observed immune activation in the carboplatin group may have resulted from an unmeasured overrepresentation of patients with tumors poised to respond to nivolumab, with carboplatin contributing little to the observed effects. It is likely that multiple factors, including our small sample size and unmeasured confounders, contributed to our findings.

There are other potential limitations to our study. On-treatment tumor biopsies were not obtained, precluding direct assessment of changes within the TME. The Olink proteomic platform can detect numerous immune-related analytes; however, in this study, only the 96-plex target panel was used providing partial coverage of immune signaling pathways. The CyTOF panel also provides only limited resolution to identify more finely differentiated but potentially important immune cell subsets. Finally, chemotherapy is known to impact systemic immune parameters beyond those assessed by our translational assays (8), which were beyond the scope of this study.

In conclusion, our study identified that between carboplatin- and oxaliplatin-containing chemo-immunotherapy regimens, the carboplatin-containing regimen was associated with a higher ORR, which also appeared greater than expected from similar trials. These findings challenge prevailing assumptions regarding the relative immunomodulatory properties of the two platinum agents and underscore the need for mechanistic and translational studies that directly compare the immunomodulatory effects of different drugs combined with PD-1/PD-L1 inhibitors in humans in an attempt to optimize combination strategies, as preclinical model systems may not accurately reflect the complex anti-tumor immune responses in patients.

Acknowledgements

Study GU16-287 was additionally supported through the Foundation for the National Institutes of Health (FNIH), in partnership with Friends of Cancer Research. Scientific and financial support for the Partnership for Accelerating Cancer Therapies (PACT) public–private partnership (PPP) are made possible through funding support provided to the FNIH by AbbVie Inc., Amgen Inc., Boehringer Ingelheim Pharma GmbH & Co. KG., Bristol Myers-Squibb, Celgene Corporation, Genentech Inc., Gilead, GlaxoSmithKline plc, Janssen Pharmaceutical Companies of Johnson & Johnson, Novartis Institutes for Biomedical Research, Pfizer Inc., and Sanofi. Additional support for investigators included P30 CA196521 (M. D. Galsky and S. Gnjatic); R01 CA24917 (M. D. Galsky); T32 CA078207 (S. Izadmehr); NIH/LRP (S. Izadmehr); U01 DK124165 and R33 CA263705 (S. Gnjatic).

Scientific and financial support for the Cancer Immune Monitoring and Analysis Centers-Cancer Immunologic Data Commons (CIMAC-CIDC) Network is provided through NCI Cooperative Agreements U24 CA224319 (to the Icahn School of Medicine at Mount Sinai CIMAC), U24 CA224331 (to the Dana-Farber Cancer Institute CIMAC), U24 CA224285 (to the MD Anderson Cancer Center CIMAC), U24 CA224309 (to the Stanford University CIMAC), and U24 CA224316 (to the CIDC at the Dana-Farber Cancer Institute), and through NCI contract 140D0421D0007 to the CIDC operated by NCI. The content is solely the responsibility of the authors and does not necessarily represent the official views of the National Institutes of Health.

This work used the services of the Tisch Cancer Institute Biorepository and Pathology Core. We thank Magdalena Thurin, Minkyung Song, and Helen Chen from NCI, Katherine Lambertson and Tetyana Murza from the FNIH, and Rebecca Enos and Rebecca Venediktov from Emmes for their support.

References

1. Galsky MD, Hahn NM, Rosenberg J, Sonpavde G, Hutson T, Oh WK, et al. A consensus definition of patients with metastatic urothelial carcinoma who are unfit for cisplatin-based chemotherapy. Lancet Oncol. England; 2011;12:211–4.
2. Dash A, Galsky MD, Vickers AJ, Serio AM, Koppie TM, Dalbagni G, et al. Impact of renal impairment on eligibility for adjuvant cisplatin-based chemotherapy in patients with urothelial carcinoma of the bladder. Cancer. United States; 2006;107:506–13.
3. Galsky MD, Hahn NM, Rosenberg J, Sonpavde G, Hutson T, Oh WK, et al. Treatment of patients with metastatic urothelial cancer “unfit” for Cisplatin-based chemotherapy. J Clin Oncol Off J Am Soc Clin Oncol. 2011;29:2432–8.
4. Galsky MD, Chen GJ, Oh WK, Bellmunt J, Roth BJ, Petrioli R, et al. Comparative effectiveness of cisplatin-based and carboplatin-based chemotherapy for treatment of advanced urothelial carcinoma. Ann Oncol Off J Eur Soc Med Oncol. 2012;23:406–10.
5. Rosenberg JE, Galsky MD, Powles T, Petrylak DP, Bellmunt J, Loriot Y, et al. Atezolizumab monotherapy for metastatic urothelial carcinoma: final analysis from the phase II IMvigor210 trial. ESMO Open. 2024;9:103972.
6. Vuky J, Balar AV, Castellano D, O’Donnell PH, Grivas P, Bellmunt J, et al. Long-Term Outcomes in KEYNOTE-052: Phase II Study Investigating First-Line Pembrolizumab in Cisplatin-Ineligible Patients With Locally Advanced or Metastatic Urothelial Cancer. J Clin Oncol. 2020;38:2658–66.
7. Collazo-Lorduy A, Galsky MD. Combining chemotherapy and immune checkpoint blockade. Curr Opin Urol. 2016;26:508–13.
8. Galluzzi L, Humeau J, Buqué A, Zitvogel L, Kroemer G. Immunostimulation with chemotherapy in the era of immune checkpoint inhibitors. Nat Rev Clin Oncol. 2020;17:725–41.
9. Hato SV, Khong A, de Vries IJM, Lesterhuis WJ. Molecular pathways: the immunogenic effects of platinum-based chemotherapeutics. Clin Cancer Res Off J Am Assoc Cancer Res. 2014;20:2831–7.
10. Carles J, Esteban E, Climent M, Font A, Gonzalez-Larriba JL, Berrocal A, et al. Gemcitabine and oxaliplatin combination: a multicenter phase II trial in unfit patients with locally advanced or metastatic urothelial cancer. Ann Oncol Off J Eur Soc Med Oncol. 2007;18:1359–62.
11. Scher HI, Armstrong AJ, Schonhoft JD, Gill A, Zhao JL, Barnett E, et al. Development and validation of circulating tumour cell enumeration (Epic Sciences) as a prognostic biomarker in men with metastatic castration-resistant prostate cancer. Eur J Cancer Oxf Engl 1990. 2021;150:83–94.
12. Simon R, Wittes RE, Ellenberg SS. Randomized phase II clinical trials. Cancer Treat Rep. 1985;69:1375–81.
13. Hoffman GE, Schadt EE. variancePartition: interpreting drivers of variation in complex gene expression studies. BMC Bioinformatics. 2016;17:483.
14. Hoffman GE, Roussos P. Dream: powerful differential expression analysis for repeated measures designs. Gorodkin J, editor. Bioinformatics. 2021;37:192–201.
15. Chen EY, Tan CM, Kou Y, Duan Q, Wang Z, Meirelles GV, et al. Enrichr: interactive and collaborative HTML5 gene list enrichment analysis tool. BMC Bioinformatics. 2013;14:128.

16. Bellmunt J, Choueiri TK, Fougeray R, Schutz FAB, Salhi Y, Winquist E, et al. Prognostic Factors in Patients With Advanced Transitional Cell Carcinoma of the Urothelial Tract Experiencing Treatment Failure With Platinum-Containing Regimens. J Clin Oncol. 2010;28:1850–5.
17. Catanzaro E, Beltrán-Visiedo M, Galluzzi L, Krysko DV. Immunogenicity of cell death and cancer immunotherapy with immune checkpoint inhibitors. Cell Mol Immunol. 2024;22:24–39.
18. Galsky MD, Arija JÁA, Bamias A, Davis ID, De Santis M, Kikuchi E, et al. Atezolizumab with or without chemotherapy in metastatic urothelial cancer (IMvigor130): a multicentre, randomised, placebo-controlled phase 3 trial. Lancet Lond Engl. 2020;395:1547–57.
19. Powles T, Csőszi T, Özgüroğlu M, Matsubara N, Géczi L, Cheng SY-S, et al. Pembrolizumab alone or combined with chemotherapy versus chemotherapy as first-line therapy for advanced urothelial carcinoma (KEYNOTE-361): a randomised, open-label, phase 3 trial. Lancet Oncol. 2021;22:931–45.
20. Galsky MD, Guan X, Rishipathak D, Rapaport AS, Shehata HM, Banchereau R, et al. Immunomodulatory effects and improved outcomes with cisplatin- versus carboplatin-based chemotherapy plus atezolizumab in urothelial cancer. Cell Rep Med. 2024;5:101393.
21. Van Der Heijden MS, Sonpavde G, Powles T, Necchi A, Burotto M, Schenker M, et al. Nivolumab plus Gemcitabine–Cisplatin in Advanced Urothelial Carcinoma. N Engl J Med. 2023;389:1778–89.
22. Powles T, Valderrama BP, Gupta S, Bedke J, Kikuchi E, Hoffman-Censits J, et al. Enfortumab Vedotin and Pembrolizumab in Untreated Advanced Urothelial Cancer. N Engl J Med. 2024;390:875–88.
23. Vogl UM, Testi I, De Santis M. Front-line Platinum Continues To Have a Role in Advanced Bladder Cancer. Eur Urol Focus. 2024;10:217–8.
24. Niegisch G. Enfortumab Vedotin and Pembrolizumab — A New Perspective on Urothelial Cancer. N Engl J Med. 2024;390:944–6.
25. He L, Kang Q, Chan KI, Zhang Y, Zhong Z, Tan W. The immunomodulatory role of matrix metalloproteinases in colitis-associated cancer. Front Immunol. 2022;13:1093990.
26. Queen A, Bhutto HN, Yousuf M, Syed MA, Hassan MI. Carbonic anhydrase IX: A tumor acidification switch in heterogeneity and chemokine regulation. Semin Cancer Biol. 2022;86:899–913.
27. Gao M, Wu X, Jiao X, Hu Y, Wang Y, Zhuo N, et al. Prognostic and predictive value of angiogenesis-associated serum proteins for immunotherapy in esophageal cancer. J Immunother Cancer. 2024;12:e006616.
28. Lewis CE, De Palma M, Naldini L. Tie2-expressing monocytes and tumor angiogenesis: regulation by hypoxia and angiopoietin-2. Cancer Res. 2007;67:8429–32.
29. Tongu M, Harashima N, Monma H, Inao T, Yamada T, Kawauchi H, et al. Metronomic chemotherapy with low-dose cyclophosphamide plus gemcitabine can induce anti-tumor T cell immunity in vivo. Cancer Immunol Immunother. 2013;62:383–91.
30. Pasquier E, Kavallaris M, André N. Metronomic chemotherapy: new rationale for new directions. Nat Rev Clin Oncol. 2010;7:455–65.

Tables

Table 1. Demographic and baseline characteristics of all randomized patients.

	Carboplatin arm N = 25*	Oxaliplatin arm N = 24*
Age, years	72 (66–81)	72 (67–78)
Sex		
Female	7 (28%)	8 (33%)
Male	18 (72%)	16 (67%)
Race		
White	21 (84%)	17 (71%)
Black or African American	2 (8%)	5 (21%)
Asian	1 (4%)	0 (0%)
Unknown	1 (4%)	2 (8%)
Tobacco use history		
Never	8 (32%)	10 (43%)
Current	1 (4%)	2 (9%)
Former	16 (64%)	11 (48%)
Unknown	0	1
Primary tumor site		
Bladder	18 (72%)	18 (78%)
Urethra	3 (12%)	2 (9%)
Renal pelvis	2 (8%)	2 (9%)
Ureters	2 (8%)	1 (4%)
Unknown	0	1
Tumor histology		
Urothelial cancer	16 (67%)	18 (78%)
Urothelial cancer with squamous features	3 (13%)	1 (4%)
Urothelial cancer with glandular features	1 (4%)	1 (4%)
Urothelial cancer with micropapillary features	2 (8%)	2 (9%)
Urothelial cancer with other variant histologies	2 (8%)	1 (4%)
Unknown	1	1
Site of metastatic disease		
Lymph node only	7 (28%)	7 (30%)
Visceral	18 (72%)	16 (70%)
Unknown	0	1
ECOG performance status		
0	9 (36%)	7 (30%)
1	11 (44%)	8 (35%)
2	5 (20%)	8 (35%)
Unknown	0	1
Creatinine clearance, mL/min	42 (37–57)	46 (37–61)
Unknown	0	1
Bellmunt score		
1	16 (64%)	16 (70%)
2	8 (32%)	6 (26%)
3	1 (4%)	1 (4%)
Unknown	0	1

*Data are median (IQR) or n (%).

Table 2. Best objective response for both treatment arms.

	Carboplatin arm N = 23	**Oxaliplatin arm N = 21**
Best Response, n (%)		
Complete Response	4 (17.4%)	2 (9.5%)
Partial Response	12 (52.2%)	5 (23.8%)
Stable Disease	4 (17.4%)	8 (38.1%)
Progressive Disease	3 (13.0%)	6 (28.6%)

Table 3. Treatment-emergent adverse events of any grade in >25% of patients and/or of grade ≥3 in >10% of patients in either group in the safety population.

Adverse Event	Carboplatin group (N = 23)*		Oxaliplatin group (N = 23)*	
	Any Grade	Grade ≥3	Any Grade	Grade ≥3
Any adverse event	23 (100%)	22 (95.7%)	23 (100%)	21 (91.3%)
Anemia	18 (78%)	8 (35%)	13 (57%)	3 (13%)
Platelet count decreased	12 (52%)	1 (4%)	18 (78%)	5 (22%)
Neutrophil count decreased	17 (74%)	12 (52%)	10 (43%)	6 (26%)
Fatigue	13 (57%)	1 (4%)	13 (57%)	0
Nausea	10 (43%)	0	14 (61%)	1 (4%)
WBC decreased	13 (57%)	4 (17%)	10 (43%)	2 (9%)
ALT increased	8 (35%)	1 (4%)	14 (61%)	1 (4%)
AST increased	6 (26%)	1 (4%)	15 (65%)	4 (17%)
Diarrhea	7 (30%)	0	14 (61%)	1 (4%)
Anorexia	5 (22%)	0	13 (57%)	0
Hypoalbuminemia	8 (35%)	0	9 (39%)	0
Creatinine increased	7 (30%)	0	9 (39%)	0
Lymphocyte count decreased	8 (35%)	3 (13%)	8 (35%)	1 (4%)
Serum amylase increased	6 (26%)	1 (4%)	10 (43%)	4 (17%)
Lipase increased	4 (17%)	3 (13%)	11 (48%)	6 (26%)
Pain	7 (30%)	2 (9%)	7 (30%)	0
Constipation	7 (30%)	0	6 (26%)	0
Peripheral sensory neuropathy	1 (4%)	1 (4%)	11 (48%)	0
Rash maculo-papular	10 (43%)	2 (9%)	2 (9%)	0
Other skin and subcutaneous tissue disorders	8 (35%)	2 (9%)	3 (13%)	0
Hyperglycemia	2 (9%)	0	9 (39%)	1 (4%)
Urinary tract infection	6 (26%)	4 (17%)	3 (13%)	1 (4%)
Fever	6 (26%)	0	3 (13%)	0
Weight loss	2 (9%)	0	6 (26%)	0
Back pain	6 (26%)	0	2 (9%)	0
Vomiting	0	0	6 (26%)	1 (4%)

*Data are n(%).

Figures Legends

Figure 1. Clinical efficacy results of the trial. **A,** Waterfall plot illustrating maximal tumor burden change from baseline for each patient. Patients who had PD as best response due to new lesion are marked with asterisks. **B–C,** Kaplan-Meier curve for PFS and OS, respectively. **D,** Swimmer plot illustrating clinical trajectory for each patient. The total length of each bar represents overall survival while the darker segment represents progression-free survival. Triangle marks the time of first documented objective response. Black rectangle marks the time of documented disease progression at any time during the study period.

Figure 2. Translational assays revealed diverging patterns of immune responses to the two platinum agents. **A,** Sample collection schema for Olink and CyTOF assay. **B–D,** Volcano plots showing the differential expression of plasma proteins on C1, C2, and C3, respectively. Baseline imbalances were adjusted for C2 and C3 data. **E–F,** Volcano plots showing the differential abundance of peripheral immune cell abundances on C1 and C3, respectively. Baseline imbalances were adjusted for C3 data. (Created in BioRender. Li, Z. https://BioRender.com/p81s2vv).

Figure 3. Associations of biomarkers with the likelihood of disease response. **A–C,** Volcano plots for likelihood of objective response based on C1, C2, and C3 Olink assay data, respectively. **D–E,** Volcano plots for likelihood of objective response based on C1 and C3 CyTOF data, respectively.

Figure 1

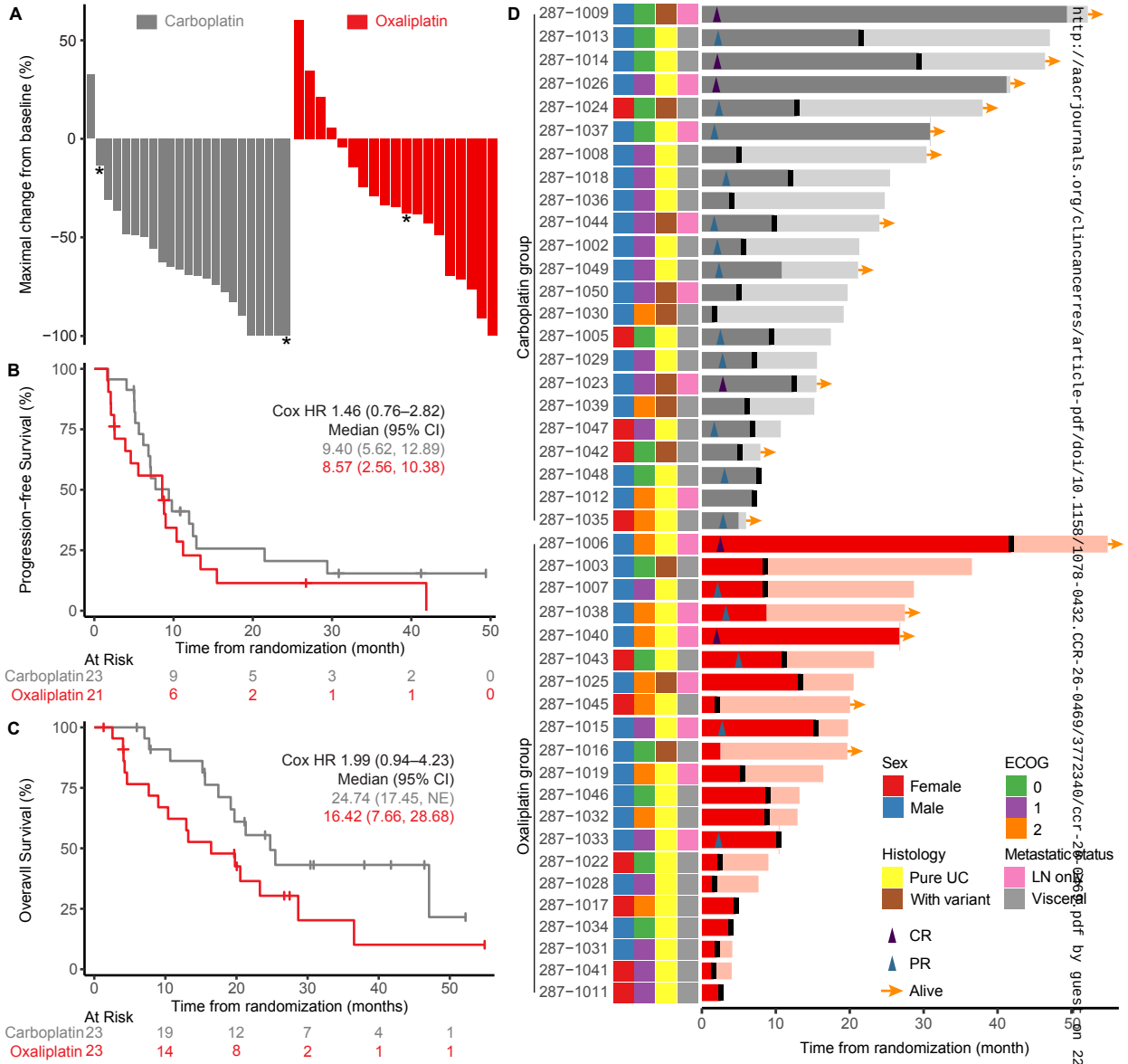

Figure 2

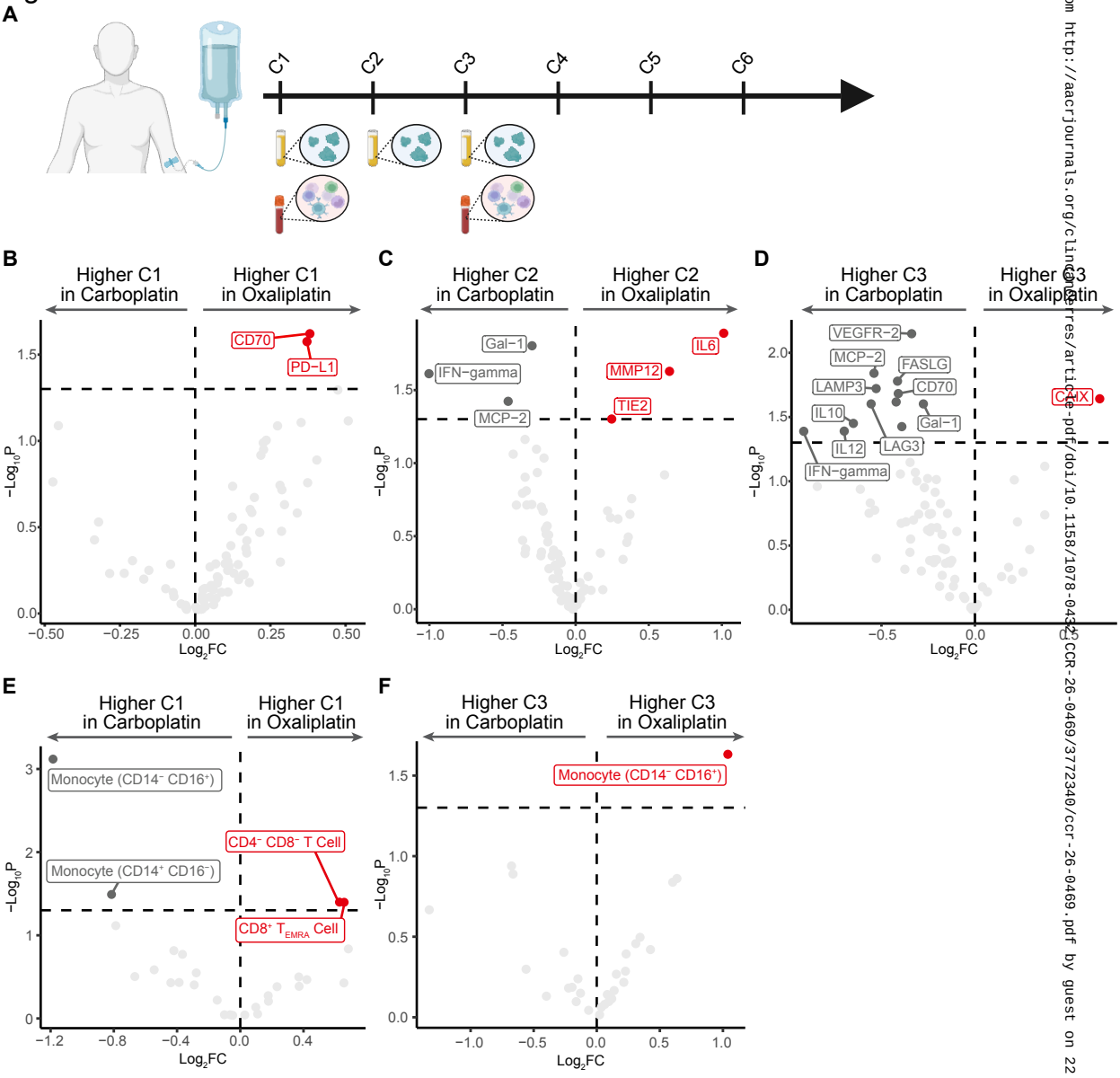

Figure 3